Electronic Supplementary Material (ESI) for Sustainable Energy & Fuels.

Electronic Supplementary Information

Sequential proton coupled electron transfers from a tetraruthenium polyoxometalate in photochemical water oxidation

Elena Rossin[a], Marcella Bonchio[a], Mirco Natali[b*], Andrea Sartorel[a*]

[a] *Department of Chemical Sciences University of Padova and Institute on Membrane Technology, Unit of Padova, via F. Marzolo 1, Padova, 35131, Italy.* andrea.sartorel@unipd.it

[b] *Department of Chemical and Pharmaceutical Sciences (DOCPAS), University of Ferrara, Via L. Borsari 46, Ferrara, 44121, Italy.* mirco.natali@unife.it

$$[Ru(bpy)_3]^{2+} + h\nu \xrightarrow{\text{step 1}} {}^*[Ru(bpy)_3]^{2+}$$

$${}^*[Ru(bpy)_3]^{2+} + S_2O_8^{2-} \xrightarrow{\text{step 2}} [Ru(bpy)_3]^{3+} + SO_4^{2-} + SO_4^{\bullet-}$$

$$[Ru(bpy)_3]^{2+} + SO_4^{\bullet-} \xrightarrow{\text{step 3}} [Ru(bpy)_3]^{3+} + SO_4^{2-}$$

$$n\,[Ru(bpy)_3]^{3+} + Ru_4POM \longrightarrow n\,[Ru(bpy)_3]^{2+} + Ru_4POM^{nOX}$$

$$Ru_4POM^{nOX} + 2\,H_2O \longrightarrow Ru_4POM^{(n-4)OX} + O_2\,4\,H^+$$

Scheme S1: Photocatalytic $[Ru(bpy)_3]^{2+}/S_2O_8^{2-}$ cycle. Photogeneration of the $[Ru(bpy)_3]^{3+}$ oxidant occurs by light absorption by $[Ru(bpy)_3]^{2+}$ (λ_{max} = 450 nm, $\varepsilon = 1.3\times10^4$ $M^{-1}cm^{-1}$) and generation of a triplet excited state $^*[Ru(bpy)_3]^{2+}$ (step 1) which activates a series of electron transfer events: reaction of $^*[Ru(bpy)_3]^{2+}$ with $S_2O_8^{2-}$ (oxidative quenching of the photosensitizer, step 2) and generation of $[Ru(bpy)_3]^{3+}$ and of a sulfate radical anion; formation of a second equivalent of $[Ru(bpy)_3]^{3+}$ by the reaction of the sulfate radical with $[Ru(bpy)_3]^{2+}$, step 3. Accumulation of oxidative equivalents on Ru_4POM catalyst follows, until the active species evolves O_2.

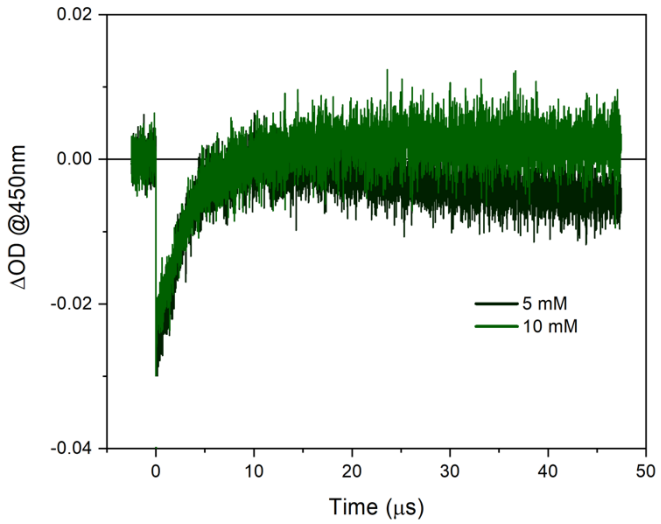

Figure S1. Kinetic traces at 450 nm obtained by laser flash photolysis of 50 μM $Ru(bpy)_3Cl_2$, 5 mM $Na_2S_2O_8$, 30 μM $Na_{10}Ru_4POM$, 0.1M Na_2SO_4 in 5–10 mM phosphate buffer at pH 2.0.

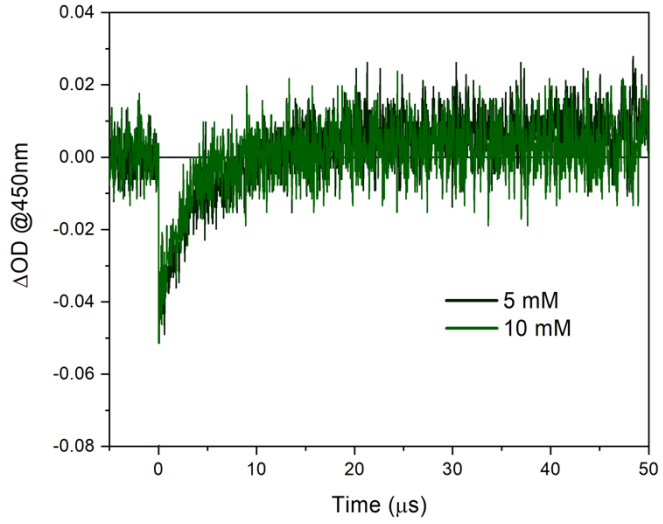

Figure S2. Kinetic traces at 450 nm obtained by laser flash photolysis of 50 μM $Ru(bpy)_3Cl_2$, 5 mM $Na_2S_2O_8$, 30 μM $Na_{10}Ru_4POM$, 0.1M Na_2SO_4 in 5–10 mM phosphate buffer at pH 4.0.

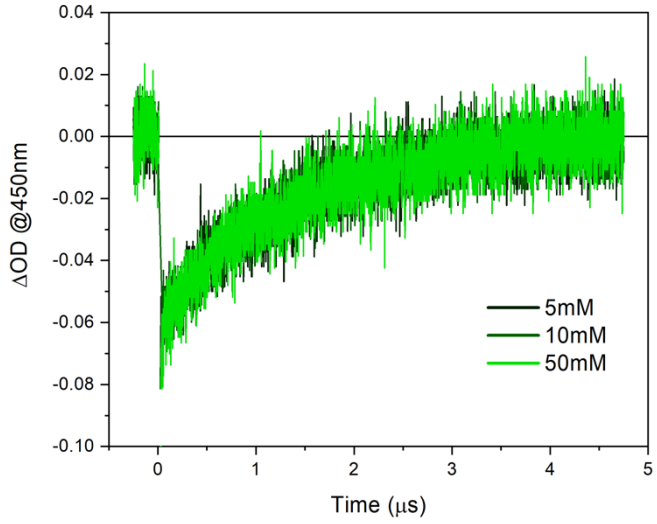

Figure S3. Kinetic traces at 450 nm obtained by laser flash photolysis of 50 μM $Ru(bpy)_3Cl_2$, 5 mM $Na_2S_2O_8$, 30 μM $Na_{10}Ru_4POM$, 0.1M Na_2SO_4 in 5–50 mM Na_2SiF_6/$NaHCO_3$ buffer at pH 5.2.

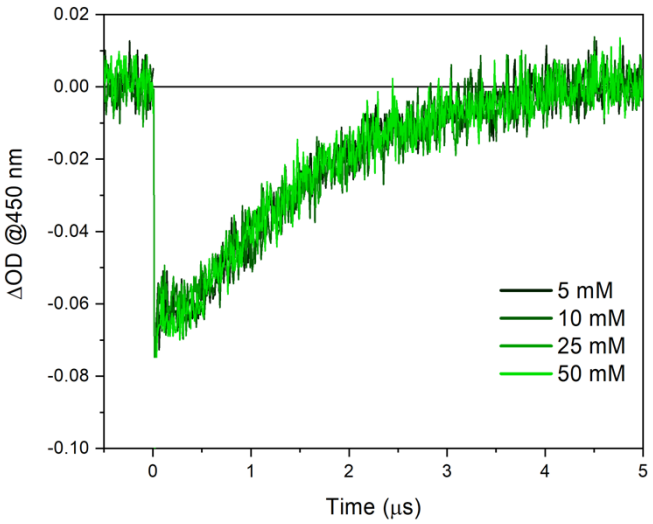

Figure S4. Kinetic traces at 450 nm obtained by laser flash photolysis of 50 µM $Ru(bpy)_3Cl_2$, 5 mM $Na_2S_2O_8$, 30 µM $Na_{10}Ru_4POM$, 0.1M Na_2SO_4 in 5–50 mM phosphate buffer at pH 6.0.

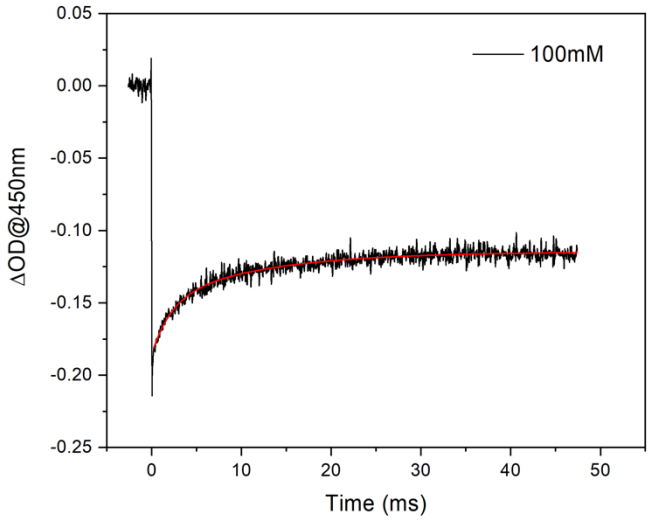

Figure S5. Kinetic trace at 450 nm obtained by laser flash photolysis of 100 µM $Ru(bpy)_3Cl_2$, 5 mM $Na_2S_2O_8$, 2.5 µM $Na_{10}Ru_4POM$, 0.1M Na_2SO_4 in 100 mM phosphate buffer at pH 6.0.

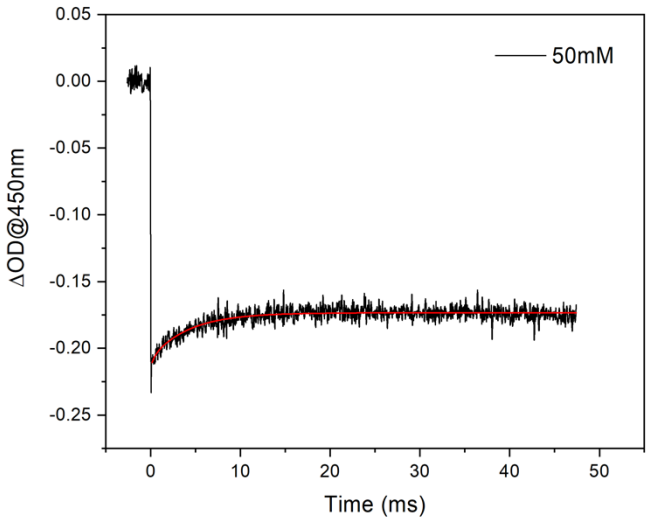

Figure S6. Kinetic trace at 450 nm obtained by laser flash photolysis of 100 µM $Ru(bpy)_3Cl_2$, 5 mM $Na_2S_2O_8$, 2.5 µM $Na_{10}Ru_4POM$, 0.1M Na_2SO_4 in 50 mM $Na_2SiF_6/NaHCO_3$ buffer at pH 5.2.

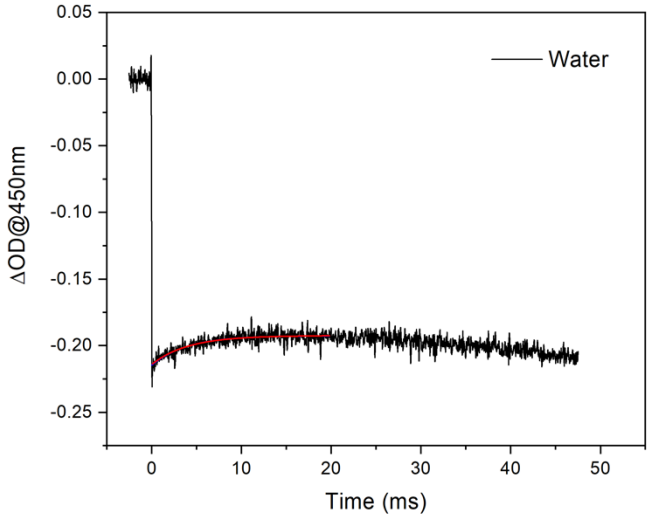

Figure S7. Kinetic trace at 450 nm obtained by laser flash photolysis of 100 µM $Ru(bpy)_3Cl_2$, 5 mM $Na_2S_2O_8$, 2.5 µM $Na_{10}Ru_4POM$, 0.1M Na_2SO_4 in water. The red line indicate a monoexponential fitting of the trace, limited to the first 20 ms.

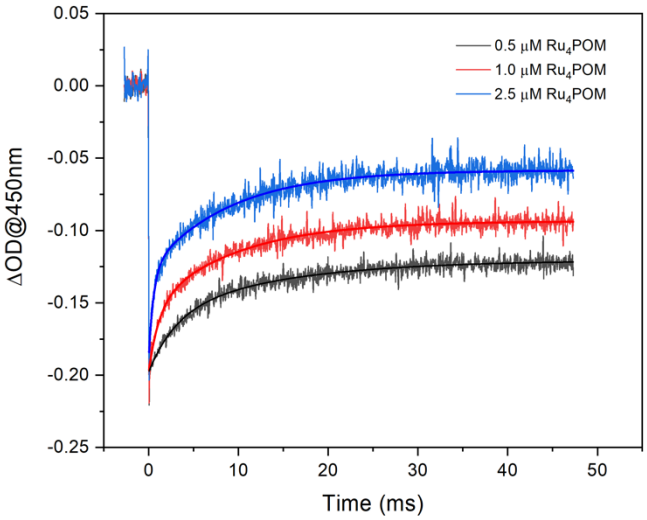

Figure S8. Kinetic traces at 450 nm obtained by laser flash photolysis of 100 µM $Ru(bpy)_3Cl_2$, 5 mM $Na_2S_2O_8$, 0.5 - 2.5 µM $Na_{10}Ru_4POM$, 0.1M Na_2SO_4 in 100 mM phosphate buffer at pH 7.0.

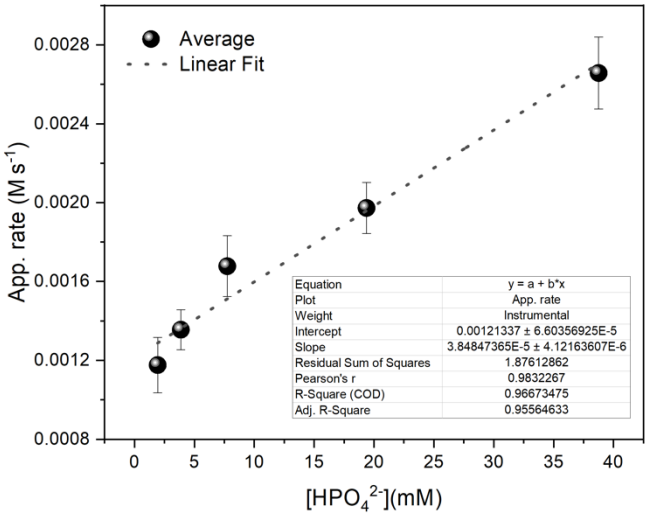

Figures S9. Plot of apparent rates for $[Ru(bpy)_3]^{3+}$ consumption (Average components) vs the concentration of HPO_4^{2-} base of the buffer.

Table S1. Average values of apparent rates for $[Ru(bpy)_3]^{3+}$ consumption at 5-100 mM phosphate buffer at pH 7.0.

Buffer (mM)	HPO_4^{2-} (mM)	Average ($M\ s^{-1}$) x 10^{-3}
5	1.93	1.18±0.1
10	3.87	1.35±0.1
20	7.75	1.68±0.2
50	19.38	1.97±0.1
100	38.76	2.66±0.2

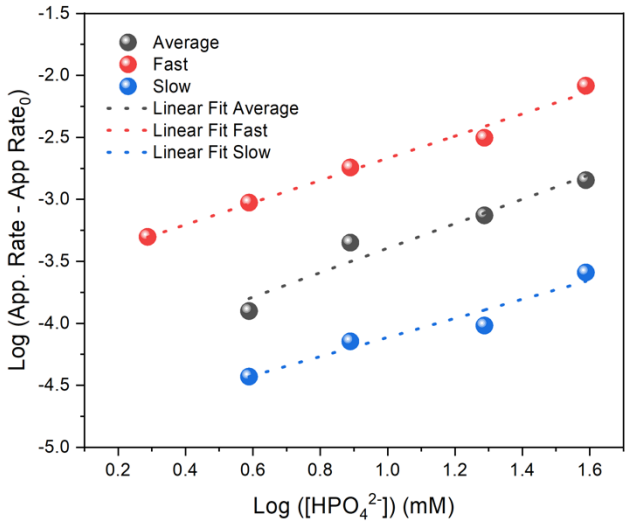

Figure S10. Log – Log plot of apparent rates for $[Ru(bpy)_3]^{3+}$ consumption (Fast, Slow and Average components, data at pH 7, see table 1 in the main text) vs the concentration of HPO_4^{2-} base of the buffer. Slopes of the linear fitting: 0.99 (Average), 0.89 (Fast), 0.77 (Slow). The LogLog analysis was performed on the following equations:

App. Rate $_{Fast}$ ($M\ s^{-1}$) = $2.62\ 10^{-3} + 2.04\ 10^{-4}\ [HPO_4^{2-}]$ (eq. 11 in the main text)

App. Rate $_{Slow}$ ($M\ s^{-1}$) = $5.45\ 10^{-4} + 6.38\ 10^{-6}\ [HPO_4^{2-}]$ (eq. 12 in the main text)

App. Rate $_{Average}$ ($M\ s^{-1}$) = $1.23\ 10^{-3} + 3.77\ 10^{-5}\ [HPO_4^{2-}]$ (from linear fitting of the data in Figure S8)

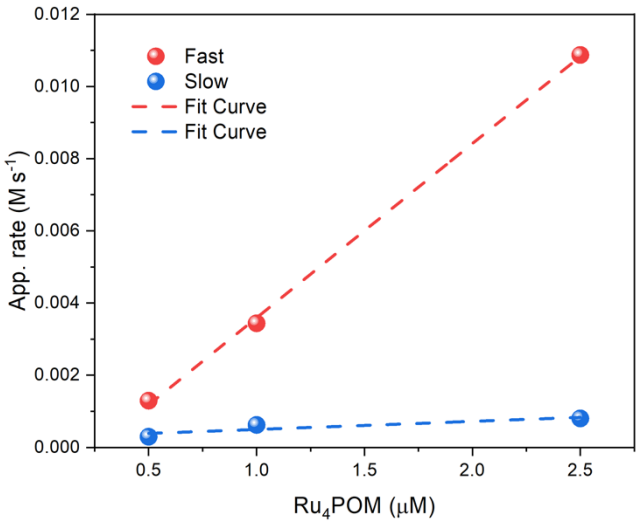

Figure S11. Plot of apparent rates for $[Ru(bpy)_3]^{3+}$ consumption (Fast and Slow components) vs the concentration of Ru_4POM.

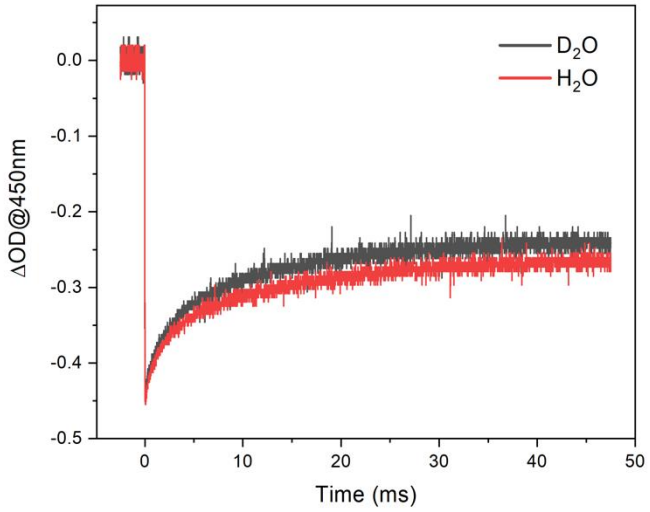

Figure S12. Kinetic traces at 450 nm obtained by laser flash photolysis of 100 µM $Ru(bpy)_3Cl_2$, 5 mM $Na_2S_2O_8$, 2.5 µM $Na_{10}Ru_4POM$, 0.1M Na_2SO_4: H/D isotopic effect at 100 mM phosphate buffer pH 7.0.

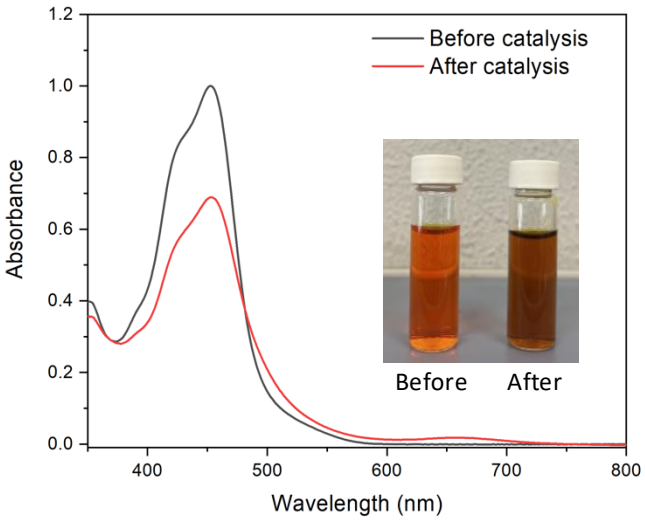

Figure S13. Absorption spectra of the reaction solution in 100 mM phosphate buffer before (black trace) and after (red trace) O_2 evolving reaction (cuvette 1mm).

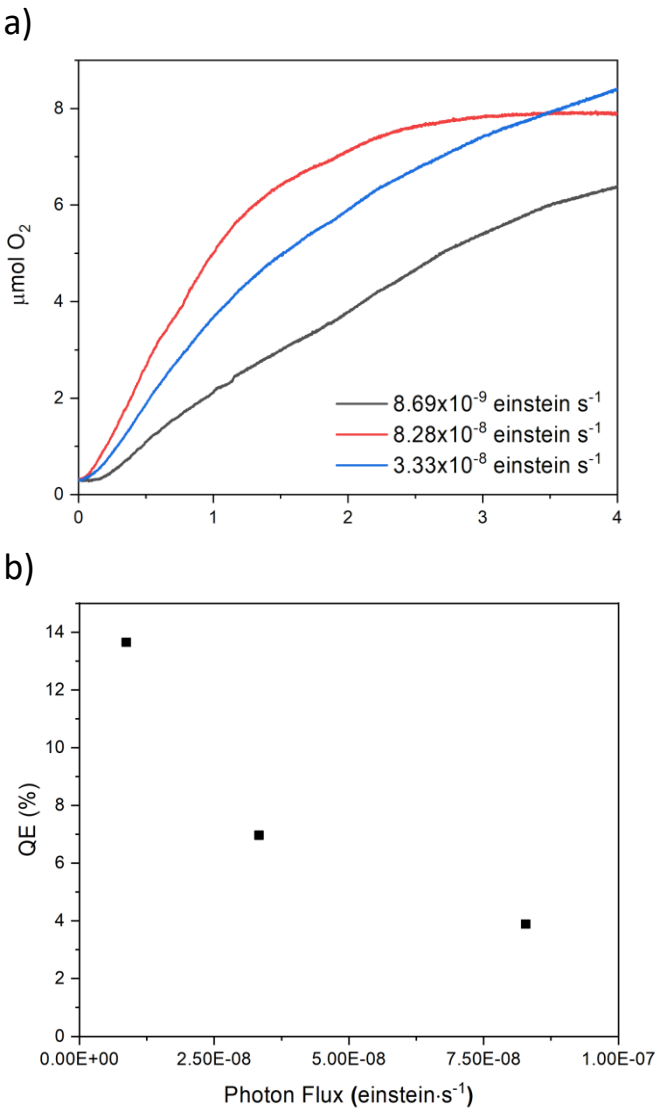

Figure S14. a) O_2 evolution traces for 15 ml solution of 1mM $Ru(bpy)_3Cl_2$, 5 mM $Na_2S_2O_8$, 5 µM $Na_{10}Ru_4POM$ at 10mM of phosphate buffer pH 7 at different power irradiation with blue led at 450 nm. b) Quantum efficiency for oxygen evolution at 10 mM phosphate pH 7, depending on the photon flux (different irradiation powers).

Kinetic model considering 6 consecutive oxidative events on Ru_4POM

The kinetic trace showing the highest reactivity of $[Ru(bpy)_3]^{3+}$ versus Ru_4POM (100 mM phosphate buffer, pH 7; purple trace in Figure 2 in the main text, top panel) was investigated with a kinetic model through computer simulations using the COPASI program. The kinetic model was conducted using the Brusselator model hypothesizing 6 consecutive oxidative events between $[Ru(bpy)_3]^{3+}$ and Ru_4POM scaffolds:

1) $[Ru(bpy)_3]^{3+} + Ru_4POM \rightarrow [Ru(bpy)_3]^{2+} + Ru_4POM^{OX}$ $k_1 = 2 \cdot 10^9\ M\ s^{-1}$ (rate constant fixed)
2) $[Ru(bpy)_3]^{3+} + Ru_4POM^{OX} \rightarrow [Ru(bpy)_3]^{2+} + Ru_4POM^{2OX}$ k_2
3) $[Ru(bpy)_3]^{3+} + Ru_4POM^{2OX} \rightarrow [Ru(bpy)_3]^{2+} + Ru_4POM^{3OX}$ k_3
4) $[Ru(bpy)_3]^{3+} + Ru_4POM^{3OX} \rightarrow [Ru(bpy)_3]^{2+} + Ru_4POM^{4OX}$ k_4
5) $[Ru(bpy)_3]^{3+} + Ru_4POM^{4OX} \rightarrow [Ru(bpy)_3]^{2+} + Ru_4POM^{5OX}$ k_5
6) $[Ru(bpy)_3]^{3+} + Ru_4POM^{5OX} \rightarrow [Ru(bpy)_3]^{2+} + Ru_4POM^{6OX}$ k_6

The results of the fitting are reported in the table below, together with the graphical representation of the experimental and fitted traces. Unfortunately, attempts of fitting the other kinetic traces in Figure 2 top panel lead to data overfitting with divergence of the rate constant values.

Parameter	**Fitted Value**
Total $[Ru_4POM]$ (being the sum of all the $[Ru_4POM]^{jOX}$ terms	2.5 μM (fixed)
Initial $[Ru(bpy)_3]^{3+}$	21 μM (fixed, obtained from the initial ΔOD, see main text)
k_1	$2 \cdot 10^9\ M\ s^{-1}$ (fixed, obtained from primary hole scavenging experiments, see main text)
k_2	$2.9 \cdot 10^8\ M\ s^{-1}$
k_3	$1.3 \cdot 10^8\ M\ s^{-1}$
k_4	$4.5 \cdot 10^7\ M\ s^{-1}$
k_5	$1.6 \cdot 10^7\ M\ s^{-1}$
k_6	$1.2 \cdot 10^7\ M\ s^{-1}$